Clinics in Diagnostic Imaging (78)

P Visrutaratna, C Sivasomboon, K Oranratanachai

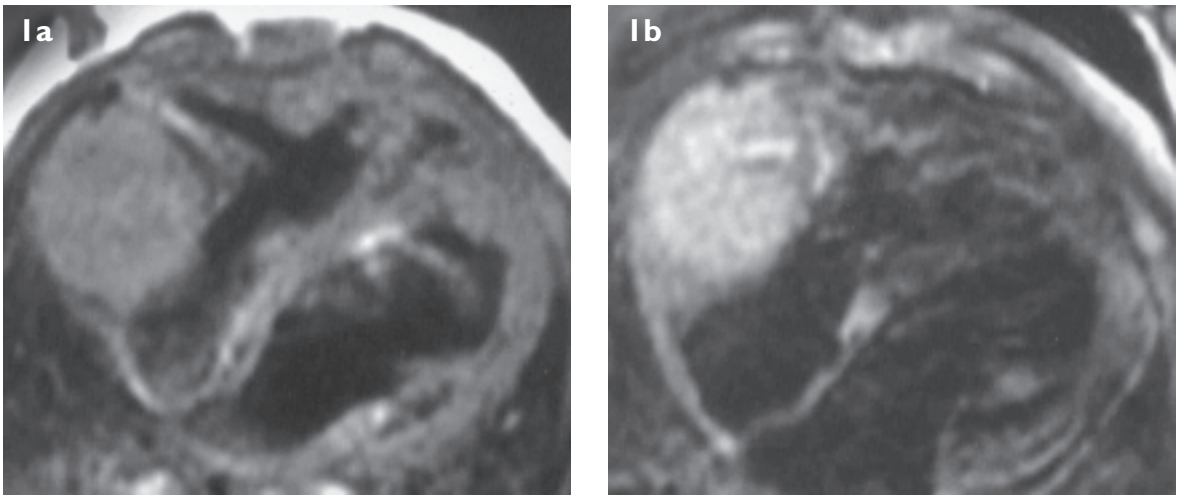

Fig. 1 Cardiac-gated axial MR images taken through the heart. (a) T1-weighted MR image. (b) T2-weighted MR image.

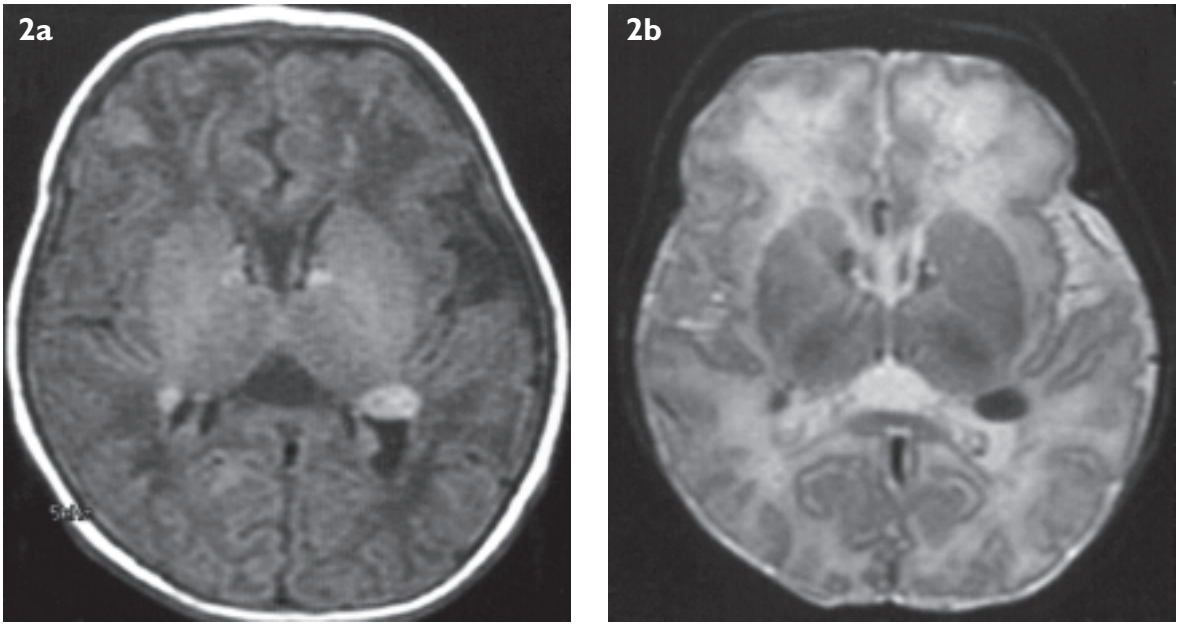

Fig. 2 Axial MR images of the brain taken at the level of the third ventricle. (a) T1-weighted MR image. (b) T2-weighted MR image.

CASE PRESENTATION

A seven-day-old boy born by caesarean section because of foetal distress was referred by another hospital for congestive heart failure. He weighed 2,600 grams at birth after a 38-week gestation. Physical examination revealed a grade III pansystolic murmur at the left lower sternal border, and ash-leaf spots on the left leg and back. Chest radiograph showed mild cardiomegaly. Echocardiography showed a 2 x 1 cm echogenic nodule at the junction of the right atrium and the right ventricle, and multiple small echogenic nodules in the right ventricle. What do the magnetic resonance (MR) images of the heart (Figs. 1a, b) and brain (Figs. 2a, b) show? What is the diagnosis?

Department of Radiology
Faculty of Medicine
Chiang Mai University
Chiang Mai 50200
Thailand

P Visrutaratna, MD
Associate Professor

C Sivasomboon, MD
Assistant Professor

K Oranratanachai, MD
Assistant Professor

Correspondence to:
Dr Pannee Visrutaratna
Tel: 66-53-945450
Fax: 66-53-217144
Email: pvisruta@mail.med.cmu.ac.th

IMAGE INTERPRETATION

The cardiac-gated axial T1-weighted MR image of the heart (Fig. 1a) shows a mass in the right atrium. The mass is isointense relative to myocardium. It is hyperintense on the axial T2-weighted MR image (Fig. 1b). The axial T1-weighted MR image of the brain (Fig. 2a) shows multiple hyperintense subependymal nodules. They are hypointense, compared with unmyelinated white matter, on the T2-weighted MR image (Fig. 2b). Two hyperintense cortical tubers are also seen on the axial T1-weighted MR image: one in the right frontal lobe and the other in the right occipital lobe. These findings are typical of cardiac rhabdomyoma, subependymal hamartomas, and cortical tubers in a newborn with tuberous sclerosis.

DIAGNOSIS

Cardiac rhabdomyoma in tuberous sclerosis.

CLINICAL COURSE

The child's father and his paternal grandfather both had tuberous sclerosis. Abdominal ultrasonography (US) showed a single cyst in the right kidney. At the age of three months, he was found to have retinal hamartomas in both eyes. Follow-up echocardiographical studies showed a decrease in the number and size of the rhabdomyomas. No cardiac mass was detectable when he was two years and eleven months old. He developed infantile spasms when he was eight months old, and has received anti-convulsant drugs since then.

DISCUSSION

Primary tumours of the heart in infants and children are extremely rare. However, an increase in the incidence of primary cardiac tumours has been reported since the development of non-invasive imaging modalities. The improve-ments in two-dimensional echocardiographical imaging and the advent of clinical cardiac MR imaging have changed the diagnostic approach to cardiac tumours. MR imaging findings complement echocardiographical findings in the investigation of children with cardiac tumours[1]. The wide field-of-view, high contrast and spatial resolution, and multiplanar imaging capabilities of MR imaging allow precise demonstration and localisation of a mass, including its anatomical relationship to the cardiac chambers and involvement of the myocardium, pericardium, or contiguous structures[2].

The types of heart tumours encountered in children differ from those seen in adults. In infants and children, the most common primary tumour of the heart is rhabdomyoma. In adults, the most common tumour is cardiac myxoma[3]. The second most common tumour in infants and children is cardiac fibroma[1,3]. Cardiac rhabdomyoma, a type of hamartoma, is usually associated with tuberous sclerosis. It is more prevalent and prominent in younger patients. 80% of children with cardiac rhabdomyoma have associated tuberous sclerosis[1]. Its frequency in patients with tuberous sclerosis has been reported from 30% in autopsies to nearly 50% in clinical series[4,5].

The clinical presentation of cardiac rhabdomyomas is diverse. In some cases, the tumour may lead to stillbirth or perinatal death. In other cases, the clinical features are usually cardiomegaly, congestive heart failure, or cardiac arrhythmias. Sudden unexpected death has also been reported. The clinical significance is determined largely by the size of the tumour, whether it is solitary or multiple, and whether or not it has expanded into a chamber cavity[3]. Cardiac rhabdomyomas usually occur in the ventricles [4-6]. Almost all rhabdomyomas are multifocal lesions, whereas cardiac fibromas are always solitary. Radiographical evidence of tumour calcification is seen in approximately 25% of patients with cardiac fibromas[2]. The characteristics of MR signal intensity of rhabdomyomas and fibromas differ. Although both masses are typically isointense relative to myocardium on T1-weighted MR images, rhabdomyomas have an increased signal intensity on T2-weighted MR images while fibromas have a decreased signal intensity[2]. Spontaneous regression of cardiac rhabdomyomas is well known[1,4- 6]. Tumours regress in size or number, or both, in most patients aged less than four years, and less so in older patients[5]. Surgery is recommended only for patients with life-threatening conditions such as refractory dysrhythmias or severe haemodynamic compromise[4,6].

Tuberous sclerosis is an autosomal dominant disease with a high mutation rate. In addition to the heart, it affects the brain, skin, kidneys, and other organs. The brain is the most commonly-involved visceral organ in tuberous sclerosis. The four most common intracranial lesions of tuberous sclerosis are cortical tubers, white matter abnormalities, subependymal nodules, and subependymal giant cell astrocytomas[7]. Astrocytoma is a low grade neoplasm while the others are hamartomas. It has been postulated that the intracranial abnormalities arise from an abnormal expression of genes within the cells of the germinal matrices of the developing brain. As a consequence, these stem cells do not differentiate, develop or migrate properly. The result is a presence of dysplastic, disorganised cells in the subependymal region, cortex, and along the curvilinear pathways between them[8]. Epilepsy and mental deficits are the

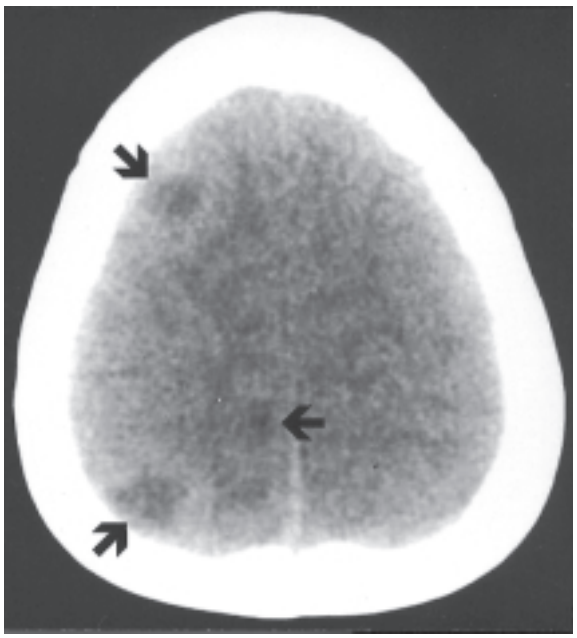

Fig. 3 Unenhanced axial CT scan of a six-year-old girl shows cortical tubers as peripheral lucencies (arrows) within broadened cortical gyri.

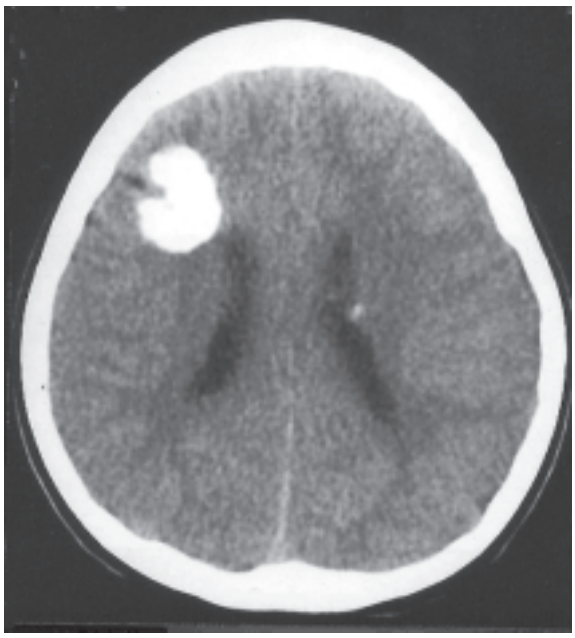

Fig. 4 Unenhanced axial CT scan of a 10-year-old girl shows a large calcified cortical tuber in the right frontal lobe and a small calcified subependymal nodule in the wall of the left lateral ventricle.

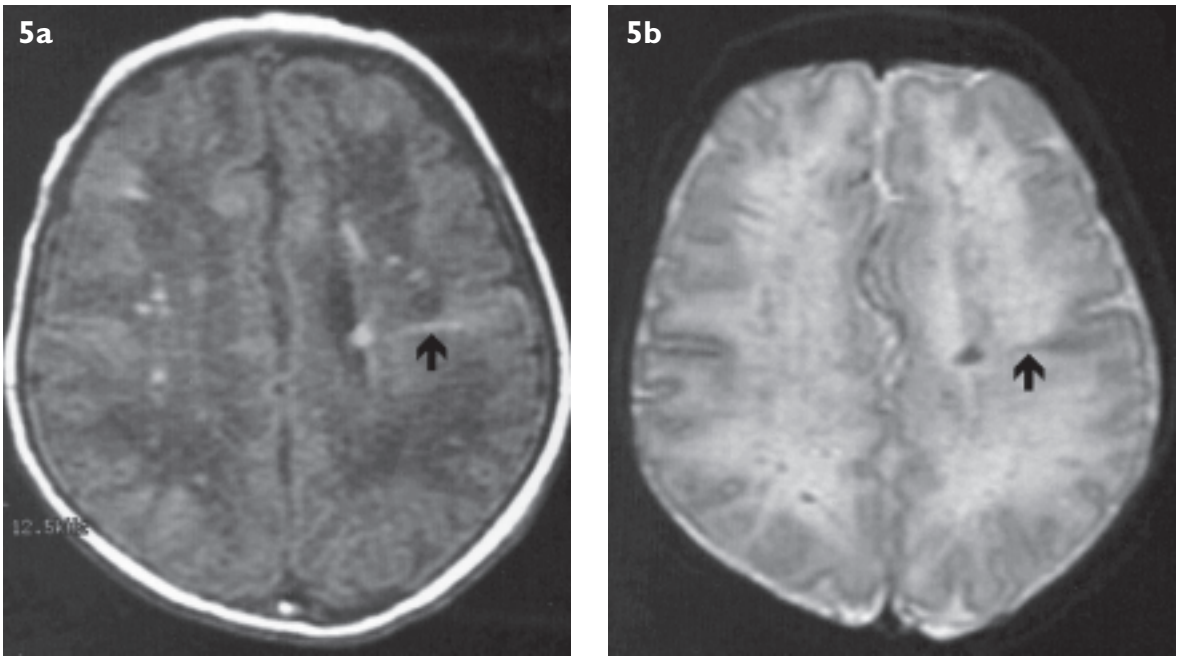

Fig. 5 White matter abnormalities in tuberous sclerosis. (a) Axial T1-weighted MR image shows multiple punctate hyperintensities in the white matter. (b) Corresponding axial T2-weighted MR image shows multiple punctate hypointensities. There is also a linear white matter lesion (arrow), which extends all the way from the wall of the left lateral ventricle to the cortex.

most common neurological problems and tend to be more severe if they manifest early[9].

In neonates and infants, the cortical tubers appear on computed tomography (CT) as peripheral lucencies within broadened cortical gyri (Fig. 3). These tend to become isodense in older children and adults. The number of calcified cortical tubers (Fig. 4) increases with age. The MR imaging appearances of cortical tubers change with age. In neonates, they appear as gyri that are hyperintense compared to white matter on T1-weighted MR images and hypointense to white matter on T2-weighted MR images. About 20% of affected gyri are enlarged[8]. In older children and adults, the peripheral component of tubers is isointense to grey matter in all pulse sequences, while the inner core of tubers is iso- to hypointense to white matter on T1-weighted MR images and hyperintense to grey and white matter on T2-weighted MR images[7].

Islets of neurons and glial cells are invariably present in the white matter of patients with tuberous sclerosis[8]. These white matter abnormalities also

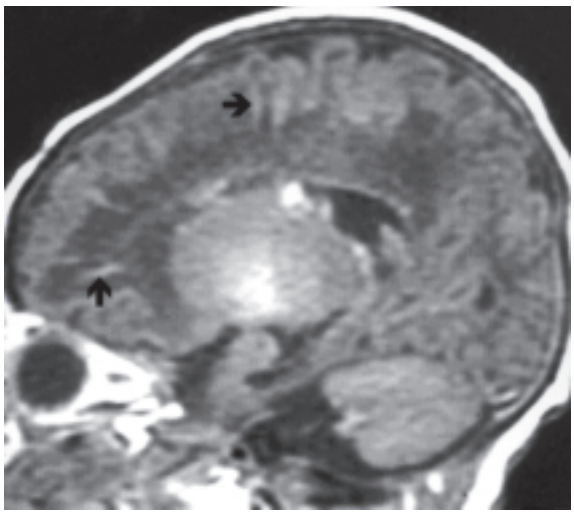

Fig. 6 Sagittal T1-weighted MR image shows multiple linear hyperintensities (arrows) in the white matter that extends in a radial pattern from the wall of the lateral ventricle to the cortex.

contain areas of hypomyelination. On CT, they appear as well-defined hypodense regions within the cerebral white matter that do not enhance. These white matter abnormalities may calcify. In neonates and young infants, these white matter abnormalities are hyperintense on T1-weighted MR images and hypointense on T2-weighted MR images. They may appear punctate (Figs. 5a, b), linear (Fig. 6), wedge-shaped, nonspecific, or tumefactive[7,9]. Diffuse signal changes affecting more than one-third of the white matter in one hemisphere have been reported[9]. The linear white matter abnormalities often extend from subependymal hamartomas to cortical tubers. These are believed to represent bands of unmyelinated, disordered cells along the pathway of the linear radial glial-neuronal unit[8]. In older patients, they may be

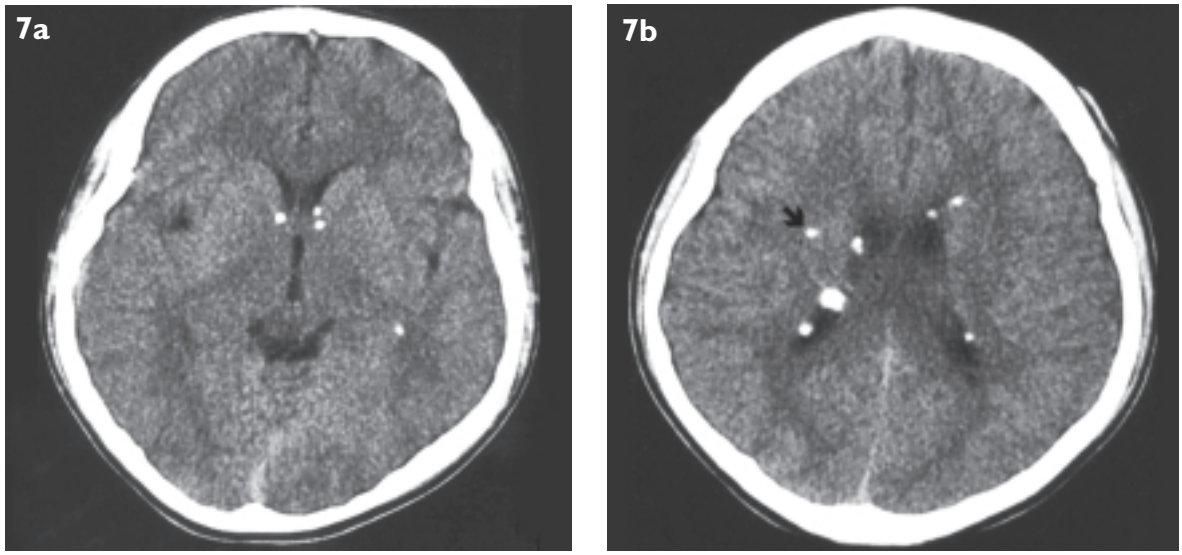

Fig. 7 Thirteen-year-old boy with multiple calcified subependymal nodules. Unenhanced axial CT scans taken through the (a) third ventricle and (b) bodies of the lateral ventricles. Note a small white matter calcification (arrow).

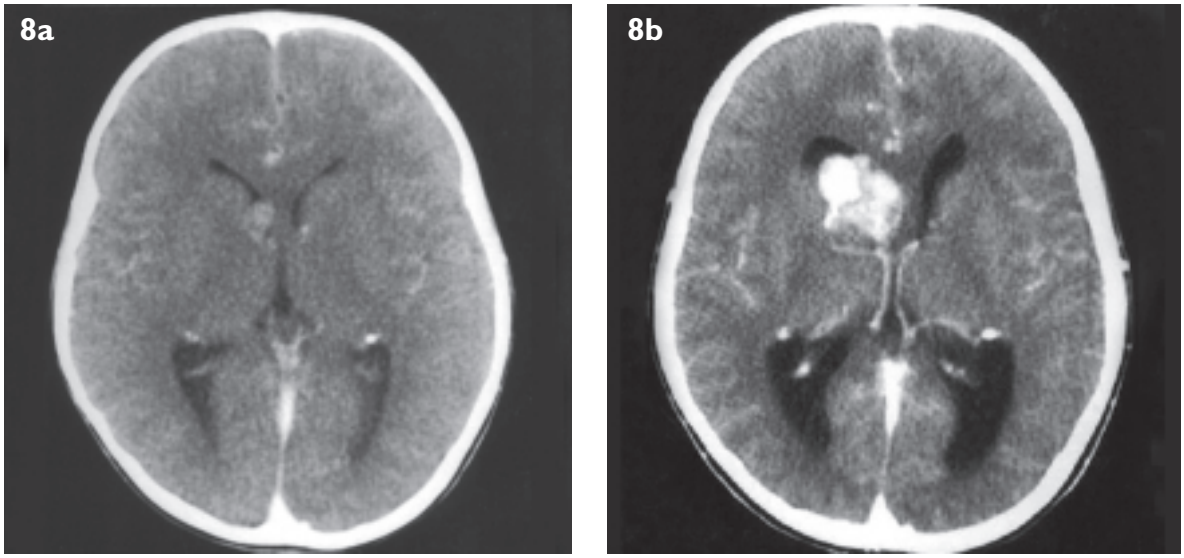

Fig. 8 Development of subependymal giant cell astrocytoma in a six-year-old girl. (a) Initial enhanced axial CT scan shows a small subependymal nodule in the wall of the right frontal horn. (b) Enhanced axial CT scan performed six years later shows marked increase in size of the subependymal nodule and dilatation of the ventricles, due to giant cell astrocytoma.

difficult to see on T1-weighted MR images and they can sometimes be identified as subtle hypointense regions. On T2-weighted MR images, they appear as well-defined hyperintense areas.

Subependymal nodules tend to be located along the ventricular surface near the caudate nucleus. The third and fourth ventricles are less frequent sites. They are rarely calcified in the first year of life. The number of calcifications typically increases with the age of the patient[8] (Figs. 7a, b). On MR images, they appear as irregular subependymal nodules that protrude into the adjacent ventricle. Their appearances change as the signal of the surrounding white matter changes[7,9]. In infants who have unmyelinated white matter, the nodules are relatively hyperintense on T1-weighted MR images and hypointense on T2-weighted MR images. In older patients, the subependymal nodules gradually become isointense compared with the white matter.

Subependymal giant cell astrocytomas are low grade neoplasms originating from the subependymal nodules and are usually situated near the foramen of Monro. Associated obstructive hydrocephalus is common. On imaging studies, they are identified by tumour growth on serial studies (Figs. 8a, b). If an enlarged contrast-enhanced nodule is seen in the subependymal region, it should be considered to be a giant cell astrocytoma[8]. Braffman et al have suggested annual or biannual cranial CT or MR examinations of patients with tuberous sclerosis during the peak age period (8-18 years) to look for occurrence of subependymal giant cell astrocytoma[7].

In the kidney, the most common lesion in patients with tuberous sclerosis is angiomyolipoma. This is found in an estimated 50 to 80 percent of patients. Another renal lesion is renal cyst which may occur alone or in conjunction with angiomyolipomas[10]. These cysts are frequently seen in children with tuberous sclerosis. Both angiomyolipomas and cysts are often bilateral and multiple but they may occur as a single lesion in one kidney. Angiomyolipomas are usually asymptomatic. However, some may cause abdominal or flank pain, haematuria, and uraemia. They may rupture, leading to retroperitoneal haemorrhage (Fig. 9) and shock. The histopathological appearance of angiomyolipomas is characterised by an admixture of mature adipose tissue, sheets of smooth muscle, and thick-walled blood vessels of various proportions[11]. Abdominal radiographs and excretory urograms may demonstrate a marked increase in renal size, and may also exhibit radiolucency associated with the fatty component of multiple angiomyolipomas[12].

On ultrasonography, an angiomyolipoma typically appears as a well-defined, hyperechoic lesion (Figs. 10a, b). Although a markedly hyperechoic lesion (isoechoic compared to the renal sinus) is highly suggestive of angiomyolipoma, this finding is not specific and therefore requires CT confirmation. The key diagnostic feature of angiomyolipoma is the presence of areas of fat attenuation within the tumour on CT (Fig. 11). Thin sections of 5 mm or less may be needed to reveal these areas[11]. A varying amount of soft tissue is also seen and determines the degree of enhancement of the lesion. On MR imaging, typical angiomyolipomas have areas of high signal intensity on T1-weighted MR

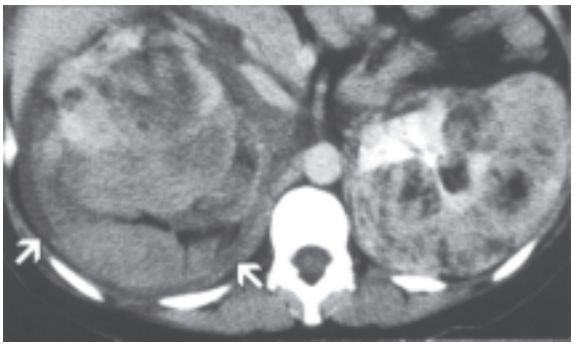

Fig. 9 Twenty-five-year-old woman with bilateral renal angiomyolipomas and rupture of angiomyolipoma in the right kidney. Enhanced axial CT scan shows large bilateral renal masses containing hypodense areas of fat interspersed with other solid elements. Note right perirenal haematoma (arrows).

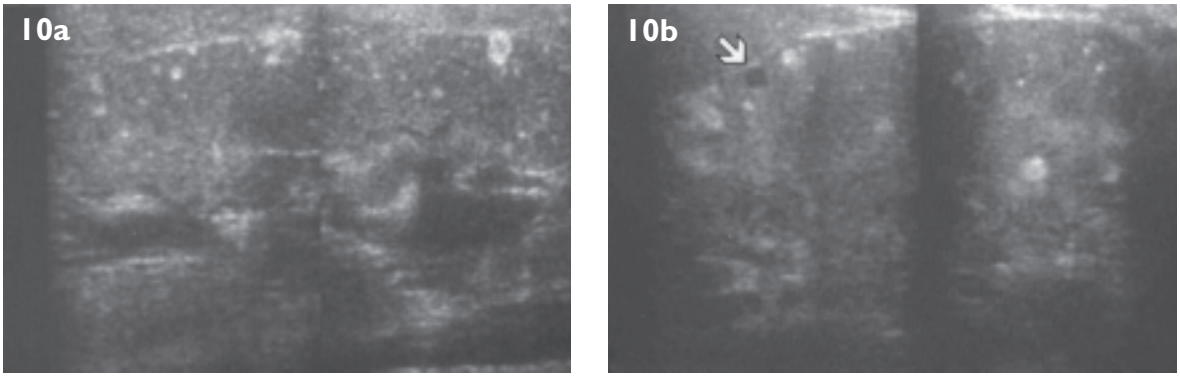

Fig. 10 Twelve-year-old girl with bilateral renal angiomyolipomas. Longitudinal US scans of the (a) right kidney and (b) left kidney show multiple tiny hyperechoic lesions. Note a small cyst (arrow) in the left kidney.

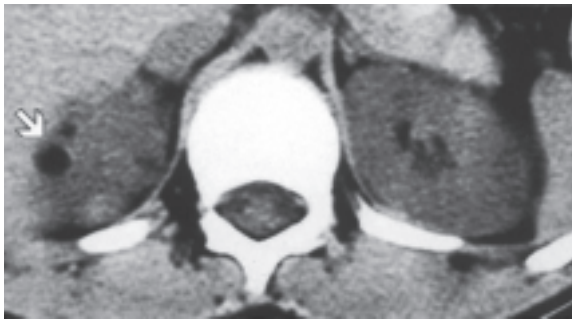

Fig. 11 Thirteen-year-old boy with right renal angiomyolipomas. Unenhanced axial CT scan shows two small masses of fat attenuation (arrow) in the upper pole of the right kidney.

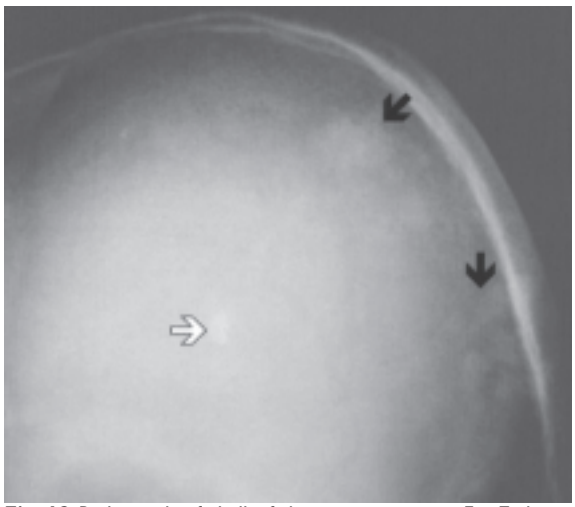

Fig. 12 Radiograph of skull of the same patient as Fig. 7 shows sclerotic lesions (black arrows) in the parietal bone. Note a small calcified subependymal nodule (white arrow).

images, with a marked decrease signal intensity with fat-suppressed sequences. However, MR imaging is usually not necessary and is less reliable than CT in the detection of small foci of fat in the tumour[11]. Angiography, which is no longer used in the diagnosis of typical fat-containing angiomyolipomas, may be needed if therapeutic embolisation is contemplated.

Lymphangioleiomyomatosis is a rare lung disease that is characterised by alveolar smooth muscle proliferation and cystic destruction of the lung parenchyma. It occurs almost exclusively in women, often between the third and fourth decades. Dyspnoea is a common presenting symptom. Pneumothoraces may also be present. The chest radiograph of these patients shows reticular, reticulonodular, miliary or honeycomb patterns. High-resolution CT scans show numerous thin-walled lung cysts surrounded by relatively normal lung parenchyma[13]. Small nodules are occasionally seen. Other organ abnormalities include sclerotic lesions of the bones (Fig. 12), multiple angiomyolipomas in the liver, and cysts and adenomas in the liver, pancreas, and spleen[14].

ABSTRACT

A seven-day-old boy with a family history of tuberous sclerosis presented with congestive heart failure. Cardiac-gated magnetic resonance (MR) imaging showed a mass in the right atrium, which was T1-isointense and T2-hyperintense relative to myocardium. Follow-up echocardiographical studies showed a decrease in the number and size of the nodules. Finally, no cardiac nodules were seen when he was two years and eleven months old. The echocardiographical studies, MR imaging findings and the clinical history are consistent with cardiac rhabdomyomas. MR imaging of the brain also showed multiple subependymal nodules, white matter abnormalities, and cortical tubers. The varied imaging appearances of tuberous sclerosis are discussed and illustrated with additional examples.

Keywords: Rhabdomyoma, Angiomyolipoma, Tuberous sclerosis, Magnetic resonance imaging

Singapore Med J 2002 Vol 43(10):541-546

REFERENCES

1. Beghetti M, Gow RM, Haney I, Mawson J, Williams WG, Freedom RM. Pediatric primary benign cardiac tumors: a 15-year review. Am Heart J 1997; 134:1107-14.
2. Grebenc ML, Rosado de Christenson ML, Burke AP, Green CE, Galvin JR. Primary cardiac and pericardial neoplasms: radiologic-pathologic correlation. Radiographics 2000; 20:1073-103.
3. Becker AE. Primary heart tumors in the pediatric age group: a review of salient pathologic features relevant for clinicians. Pediatr Cardiol 2000; 21:317-23.
4. Bosi G, Lintermans JP, Pellegrino PA, Svaluto-Moreolo G, Vliers A. The natural history of cardiac rhabdomyoma with and without tuberous sclerosis. Acta Paediatr 1996; 85:928-31.
5. Nir A, Tajik AJ, Freeman WK, Seward JB, Offord KP, Edwards WD, et al. Tuberous sclerosis and cardiac rhabdomyoma. Am J Cardiol 1995; 76:419-21.
6. Smythe JF, Dyck JD, Smallhorn JF, Freedom RM. Natural history of cardiac rhabdomyoma in infancy and childhood. Am J Cardiol 1990; 66:1247-9.
7. Braffman BH, Bilaniuk LT, Naidich TP, Altman NR, Post MJ, Quencer RM, et al. MR imaging of tuberous sclerosis: pathogenesis of this phakomatosis, use of gadopentetate dimeglumine, and literature review. Radiology 1992; 183:227-38.
8. Barkovich AJ. Pediatric Neuroimaging. 3rd ed. Philadelphia: Lippincott Williams & Wilkins, 2000.
9. Baron Y, Barkovich AJ. MR imaging of tuberous sclerosis in neonates and young infants. AJNR 1999; 20:907-16.
10. Stillwell TJ, Gomez MR, Kelalis PP. Renal lesions in tuberous sclerosis. J Urol 1987; 138:477-81.
11. Helenon O, Merran S, Paraf F, Melki P, Correas JM, Chretien Y, et al. Unusual fat-containing tumors of the kidney: a diagnostic dilemma. Radiographics 1997; 17:129-44.
12. Davidson AJ, Hartman DS, Choyke PL, Wagner BJ. Davidson s radiology of the kidney and genitourinary Tract. 3rd ed. Philadelphia: WB Saunders, 1999.
13. Webb WR, M ller NL, Naidich DP. High-Resolution CT of the Lung. Philadelphia: Lippincott Williams & Wilkins, 2001.
14. Evans JC, Curtis J. The radiological appearances of tuberous sclerosis. Br J Radiol 2000; 73:91-8.